J. Hydrol. Hydromech., 69, 2021, 1, 108–118
DOI: 10.2478/johh-2020-0041
ISSN 1338-4333

sciendo Journal of Hydrology and Hydromechanics

Effect of debris accumulation on scour evolution at bridge pier in bank proximity

Michele Palermo[1*], Simone Pagliara[2], Deep Roy[1]

[1] DESTEC - Department of Energy, Systems, Territory and Construction Engineering, University of Pisa, Via Gabba 22, Pisa 56122, Italy.
E-mails: michele.palermo@ing.unipi.it; d.roy1@studenti.unipi.it
[2] Department of Civil and Environmental Engineering, Imperial College London, South Kensington, London SW7 2AZ, UK.
E-mail: simo.pagliara@gmail.com
[*] Corresponding author. Tel.: 0039 050 2217929. E-mail: michele.palermo@ing.unipi.it

Abstract: Large debris transported by flood affects scour features at bridge piers and increases the risks of structural failure. Geometric characteristics of the debris and the relative position of the pier with respect to the river bank are important parameters for the scour process. The interaction between the water flow and debris accumulation increases the shear stress, turbulence and consequently enhances the scour depth at the pier. This paper aims at analyzing such effects on scour evolution at bridge piers. To this end, two series of tests were carried out under clear water condition with different debris geometries and percentage blockage ratios. Experimental evidences showed that the pier position only influences scour evolution and equilibrium morphology for low water depths. Conversely, its effect becomes negligible for scour at bridge piers with debris accumulation and higher water depths. Useful practical relationships have been derived, with satisfactory prediction capability of the scour evolution for all the tested configurations.

Keywords: Hydraulic model; Large debris; Local scour; Time evolution.

INTRODUCTION

Large debris (LD) accumulation represents a key aspect in scour related problems at bridge piers that should be carefully taken into consideration for a correct design of the structure and realistic assessment of the scour mechanism. LD accumulation determines flow obstruction and results in a significant modification of velocity field in correspondence with the bridge pier. Consequently, both shear stress acting on the bed material and lift action in the pier wake region significantly vary, enhancing the chances of failure due to an increase of the scour hole geometric characteristics.

The catastrophic 1993 upper Mississippi river basin flood is an example of the high damage capacity of floods on bridge pier (Hagerty et al., 1995). In fact, the main cause of bridge failures was due to accumulation of debris on secondary roadway bridges. Therefore, debris accumulation at the bridge piers assumes a fundamental importance and requires further investigations in order to optimize bridge pier design and increase bridge resilience.

Bridge pier scour is a topic that has been deeply studied over the last decades. Specifically, many researchers investigated scour process in correspondence with bridge piers, providing useful insights on its mechanism and empirical (or semi-theoretical) relationships to predict the maximum scour depth. Among others, Chiew (1995), Franzetti et al. (1994), Kandasamy and Melville (1998), Laursen (1958), Masjedi et al. (2010), Melville and Sutherland (1988), Raikar and Dey (2008), Raudkivi and Ettema (1985), Richardson and Davis (2001), Shen et al. (1969) and Tang et al. (2009) analyzed the scour phenomenon and evidenced the main parameters governing the scour process. Some of the mentioned studies also focused on effective countermeasures to limit its extension (e.g., collars, rip rap, sills, etc.). Overall, Melville (1997), Sheppard (1999) and Zarrati et al. (2010) showed the role of several key parameters influencing the scour process, e.g., the approaching water depth h, the pier diameter D, the flow intensity U/U_c, where U indicates the average approach flow velocity and U_c is the critical flow velocity, and bed material mean diameter d_{50}.

Other studies also focused on scour evolution, highlighting that scour depth increases up to reach an asymptotic value at the equilibrium condition (Barbhuiya and Dey, 2003; Chang et al., 2004; Dey, 1999; Dey and Barbhuiya, 2005; Franzetti et al., 1989; Kothyari et al., 1992; Link et al., 2008; Melville and Chiew, 1999; Melville and Coleman, 2000; Oliveto and Hager, 2002, 2005; Zevenbergen, 2000).

More recently, the effect of logs and woody debris on the river morphology and flow deflection has been investigated (among others, Abbe and Montgomery, 2003; Andreoli et al., 2007; Braudrick and Grant, 2001; Gurnell et al., 2002; Wallerstein and Thorne, 1996). Nevertheless, these studies focused on the accumulation in rivers and creek beds rather than at bridge piers. Lyn et al. (2003) studied the hydraulic mechanism of LD accumulation at bridge crossing. They showed that the relative dimension of the logs with respect to the depth of water is a crucial parameter in determining debris trapping potential.

Nevertheless, only a few studies provide design procedures to assess the influence of debris accumulation on the bridge pier scour. In particular, Melville and Dongol (1992) conducted a series of experimental tests using a cylindrical accumulation extending downstream of the bridge pier. The influence of the accumulation on the scour hole was observed and useful practical relationships were developed involving the concept of equivalent bridge pier diameter. Furthermore, Diehl (1997) found that debris accumulation is one of the major factors behind bridge failures in the USA, because of the increased flow obstruction due to sediment accumulation, modified angle of attack deflection and discharge capacity of the bridge (Kattell and Eriksson, 1998). Successively, Mueller and Parola (1998) and Parola et al. (1998) investigated the flow field pier scour in the presence of debris accumulation and highlighted the significant variations with respect to the case of isolated pier. They showed that hydrodynamic forces depend on debris frontal shapes, accumulation roughness, porosity and blockage ratio (see also Bradley et al., 2005; Briaud et al., 2006; Parola et al., 2000; Zevenbergen et al., 2006).

More recently, Pagliara and Carnacina (2010) and (2011) investigated the effects of debris roughness and shape on scour evolution. They found that the scour mechanism is slightly affected by debris roughness and provided empirical relationships to estimate scour hole geometry. They validated their formulas by using a large database, including data of other authors obtained under different hydraulic conditions.

Although numerous studies have been conducted on the topic, the effect of the distance of the bridge pier from the channel wall on the scour evolution is still underexplored. Apparently, no studies are present in the open literature dealing with such effect in the presence of LD accumulation in correspondence with an isolated pier. Therefore, new experimental tests were conducted to fill this gap of knowledge. More specifically, two series of tests were carried by varying the distance of a single bridge pier from the channel wall, both in the presence and absence of LD accumulation. Experimental tests evidenced that scour depth decreases with distance from channel wall for isolated piers (reference configuration), while it increases with LD accumulation for any pile position with respect to the corresponding reference configuration. Useful empirical equations are proposed to estimate the scour depth evolution for all the tested configurations.

MATERIALS AND METHODS

Experimental tests were carried on in a glass-walled, horizontal channel 7.6 m long, 0.61 m wide and 0.5 m deep. Flow discharge was measured by means of a KROHNE® Optiflux 2000 electromagnetic flow sensor. The discharge was supplied by means of a sluice gate provided with a flow straightener. The bridge pier was simulated using a plexiglass cylinder with diameter D. The flow depth in the channel was regulated by a movable weir located at its end and it was kept constant during tests. The movable bed was simulated by using a sand material, whose granulometric characteristics are: d_{50} = 1.0 mm, σ = 1.2 and ρ_s = 2440 kg/m^3, where d_{50} is the mean diameter, σ is the non-uniformity coefficient and ρ_s is the sediment density. According to Melville and Chiew (1999), Oliveto and Hager (2005), Raudkivi and Ettema (1983) and (1985) bed forms do not occur for the tested channel bed material, as well as cohesive and armoring effects are assumed to be negligible (d_{50} > 0.9 mm and σ < 1.3, respectively). Furthermore, the sediment entrainment velocity U_c and the Shields' parameter θ were estimated by adopting the criterium proposed by Wu and Wang (1999). Namely, following such approach, it is possible to estimate the critical shear velocity u^*_c and the energy line slope i_c. Then, using Manning's formula with a Strickler coefficient $n = 0.047d_{50}^{1/6}$, U_c can be evaluated. The predicting capability of such approach was also tested by Pagliara and Carnacina (2010) who conducted experiments in the absence of the pier, resulting in a good agreement between observations and predictions. All the tests were conducted by keeping the ratio constant at $U/U_c \approx 1$, as, for uniform bed materials and under clear-water conditions, the maximum scour depth occurs for $U \approx U_c$ (Melville, 1997).

Two series of experimental tests were conducted. The first series consisted of 25 reference tests, which were carried out in the absence of any LD accumulation. Namely, these tests were conducted using two pier diameters (D = 0.03 m and 0.04 m) by varying the non-dimensional distance of the pier axis from the channel wall in the range $1/12 \le p_p/b \le 1/2$, where p_p indicates the distance of the pier axis from the channel wall and b is the channel width. The choice of the two pier diameters adopted in this study was based on previous findings of other authors. Namely, according to Oliveto and Hager (2002), the effect of D/b on the maximum scour depth is negligible for D/b<0.1. In addition, Pagliara and Carnacina (2010) showed that the effect of the parameter D/d_{50} can be neglected in the tested conditions. Figure 1 shows six views (planar, side and frontal) of a pier located symmetrically and asymmetrically in the channel, respectively, along with the main geometric and hydraulic parameters. z_{max} indicates the maximum scour depth, and l_d, d_d and t_d are debris longitudinal length, width and submerged height, respectively. For each test, channel bed was carefully levelled and slowly filled up until reaching the desired water depth. Water flow could enter the channel very slowly, to avoid scour around the pier during hydraulic conditions set-up. Then, the target discharge Q was set and the water depth h at a distance of 0.5b upstream of the pier axis was measured and kept constant by regulating the downstream sluice gate (Oliveto and Hager, 2002; Melville and Dongol, 1992). This instant was considered as the test beginning (t = 0 s). During every test, z_{max} always occurred in correspondence with the upstream side of the pier, regardless of the pier diameter and position in the channel, and was surveyed by means of a ±0.5 mm precise clear scales glued on both the sides of the pier. For each test, z_{max} measurements were taken at t = 1, 2, 4, 8, 15, 30, 60, 90, 120 minutes from the test beginning and, subsequently, after every 1-hour up to the selected test duration t^* (generally ranging between 6 and 8 hours, see Table 1).

Table 1. Summary of experimental tests conducted without inclusion of LD.

Test	D (cm)	p_p/b (–)	Q (l/s)	h/D (–)	z_{max} (cm)	t^* (hour)
1	3	1/2	33.50	5.67	5.50	7.5
2	3	1/4	33.50	5.67	5.70	8
3	3	1/4	17.00	2.67	5.80	6
4	3	1/12	17.00	2.67	6.20	6
5	3	1/12	33.50	5.67	5.90	7
6	3	1/12	8.00	1.40	4.50	6
7	3	1/6	17.00	2.67	6.10	6
8	4	1/2	17.00	2.00	6.90	6
9	4	1/2	33.50	4.25	7.20	6
10	4	1/12	17.00	2.00	8.20	6
11	4	1/12	8.00	1.05	6.00	6
12	4	1/12	33.50	4.25	7.30	6
13	4	1/2	8.00	1.05	5.20	6
14	4	1/6	8.00	1.05	5.90	6
15	4	1/6	17.00	2.00	7.00	6
16	4	1/6	33.50	4.25	6.70	6
17	3	1/2	8.00	1.40	4.80	6
18	3	1/2	17.00	2.67	6.50	6
19	3	1/4	17.00	2.67	7.20	72
20	3	1/6	17.00	2.67	6.10	6
21	3	1/6	8.00	1.40	4.70	6
22	3	1/6	33.50	5.67	5.50	6
23	3	1/2	33.50	5.67	4.30	6
24	3	1/2	17.00	2.67	5.10	6
25	3	1/2	8.00	1.40	4.20	6

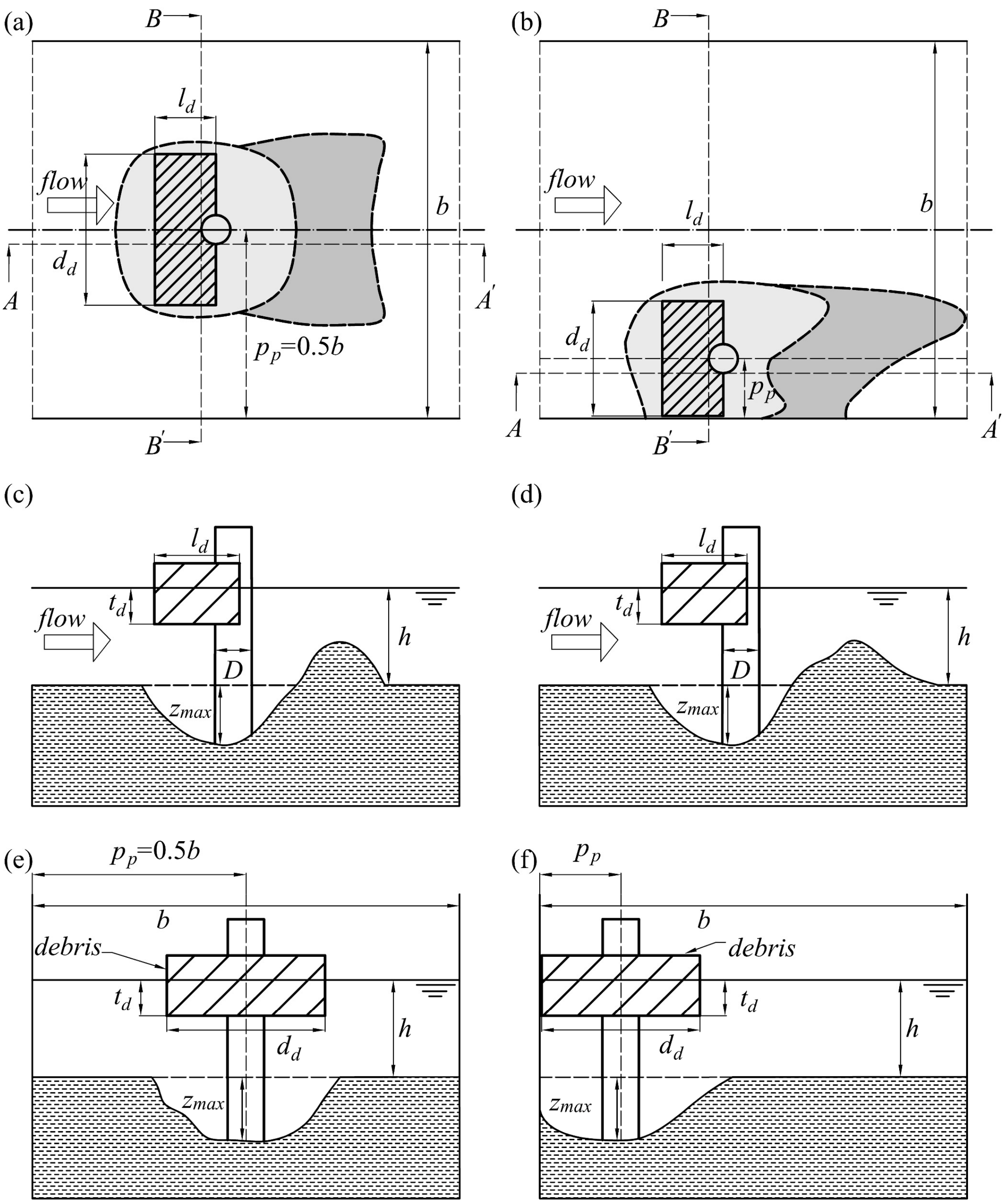

Fig. 1. Diagram sketch of the experimental apparatus along with the main hydraulic and geometric parameters: planar views of a pier located **(a)** symmetrically and **(b)** asymmetrically; side views (section A–A′) of a pier located **(c)** symmetrically and **(d)** asymmetrically; and frontal views (section B-B′) of a pier located **(e)** symmetrically and **(f)** asymmetrically.

The selected test duration t^* allowed us to reach equilibrium condition for the adopted channel bed material (Pagliara and Carnacina, 2010, 2011). This occurrence was further verified by conducting a special test of longer duration (test 19 in Table 1, $t^* = 72$ hours). In this regard, it is worth mentioning that the difference between the maximum scour depths at $t^* = 6$ and 72 hours was approximately equal to 4%, that is negligible in terms of practical applications. At the end of each test, channel bed morphology was surveyed by using a ±0.1 mm precise point gauge.

The second series of experiments consisted of 56 tests (Table 2) and was conducted to investigate the effect of LD accumulation for a bridge pier asymmetrically located in the channel. Namely, tests with pier diameter $D = 0.03$ m were conducted in the presence of LD accumulation simulated by using two different plexiglass boxes (Type A and B, respectively). Type A was characterized by the following geometric dimensions: $l_d = 0.15$ m, $d_d = 0.2$ m, and debris height $h_d = 0.09$ m; whereas, for Type B, $l_d = 0.09$ m, $d_d = 0.17$ m and $h_d = 0.16$ m. Also, the channel set-up and measurement methodology were the same as described above, as well as the adopted bed material. Tests were conducted for p_p/b ranging between 1/6 and 1/2 and t^* between 6 and 22.3 hours. According to Pagliara and Carnacina (2010) and Pagliara et al. (2015), the percentage blockage ratio $\Delta A = 100[(d_d–D)t_d]/(bh)$ varied between 6 and 18%. Figure 2 shows two pictures of test 55. Table 2 summarizes the values of the main parameters characterizing the second series of tests.

Table 2. Summary of experimental tests conducted with inclusion of LD.

Test	D (cm)	p_p/b (–)	Q (l/s)	h/D (–)	z_{max} (cm)	t^* (hour)	Debris type	ΔA (%)
26	3	1/2	17.00	2.67	7.30	6.0	B	6.00
27	3	1/2	8.00	1.40	7.00	6.0	B	6.00
28	3	1/4	17.00	2.67	7.90	6.0	B	6.00
29	3	1/4	33.00	5.67	7.20	6.0	B	6.00
30	3	1/4	8.00	1.40	4.50	6.0	B	6.00
31	3	1/4	17.00	2.67	9.90	6.0	B	12.00
32	3	1/4	33.00	5.67	10.20	6.0	B	12.00
33	3	1/4	8.00	1.40	8.00	6.0	B	12.00
34	3	1/4	17.15	2.67	11.00	6.0	B	18.00
35	3	1/4	8.00	1.40	7.70	6.0	B	18.00
36	3	1/4	33.00	5.67	11.50	6.0	B	18.00
37	3	1/4	17.00	2.67	8.10	6.0	A	6.00
38	3	1/4	8.00	1.40	5.70	6.0	A	6.00
39	3	1/4	33.00	5.67	8.10	6.0	A	6.00
40	3	1/4	17.00	2.67	8.30	6.0	A	12.00
41	3	1/4	8.00	1.40	6.20	6.0	A	12.00
42	3	1/4	17.00	2.67	9.70	6.0	A	18.00
43	3	1/4	8.00	1.40	6.40	6.0	A	18.00
44	3	1/4	33.50	5.67	9.70	6.0	A	12.00
45	3	1/4	33.50	5.67	9.60	6.0	A	14.75
46	3	1/6	17.00	2.67	7.00	6.0	B	6.00
47	3	1/6	33.50	5.67	8.10	6.0	B	6.00
48	3	1/6	8.00	1.40	4.90	6.0	B	6.00
49	3	1/6	17.00	2.67	9.60	6.0	B	12.00
50	3	1/6	33.50	5.67	11.00	6.0	B	12.00
51	3	1/6	8.00	1.40	6.70	6.0	B	12.00
52	3	1/6	17.00	2.67	12.20	6.0	B	18.00
53	3	1/6	8.00	1.40	7.10	6.0	B	18.00
54	3	1/6	33.50	5.67	13.50	6.0	B	18.00
55	3	1/6	17.00	2.67	8.00	6.0	A	6.00
56	3	1/6	8.00	1.40	7.00	6.0	A	6.00
57	3	1/6	33.50	5.67	8.10	6.0	A	6.00
58	3	1/6	17.00	2.67	11.30	6.0	A	12.00
59	3	1/6	33.50	5.67	10.70	6.0	A	12.00
60	3	1/6	8.00	1.40	6.30	6.0	A	12.00
61	3	1/6	17.00	2.67	10.80	6.0	A	18.00
62	3	1/6	8.00	1.40	6.80	4.0	A	18.00
63	3	1/6	33.50	5.67	10.20	6.0	A	15.00
64	3	1/2	33.50	5.67	7.40	22.3	B	6.00
65	3	1/2	33.50	5.67	10.70	20.4	B	12.00
66	3	1/2	33.50	5.67	10.40	6.0	B	18.00
67	3	1/2	17.00	2.67	9.40	21.4	B	6.00
68	3	1/2	17.00	2.67	12.30	22.4	B	12.00
69	3	1/2	17.00	2.67	11.00	6.0	B	18.00
70	3	1/2	8.00	1.40	7.80	21.5	B	6.00
71	3	1/2	8.00	1.40	9.00	21.6	B	12.00
72	3	1/2	8.00	1.40	5.60	6.0	B	18.00
73	3	1/2	33.50	5.67	7.00	21.2	A	6.00
74	3	1/2	33.50	5.67	7.40	6.0	A	12.00
75	3	1/2	33.50	5.67	10.60	6.0	A	18.00
76	3	1/2	17.00	2.67	9.50	21.4	A	6.00
77	3	1/2	17.00	2.67	9.00	6.0	A	12.00
78	3	1/2	17.00	2.67	10.60	6.0	A	18.00
79	3	1/2	8.00	1.40	7.60	21.4	A	6.00
80	3	1/2	8.00	1.40	6.80	6.0	A	12.00
81	3	1/2	8.00	1.05	6.20	6.0	A	18.00

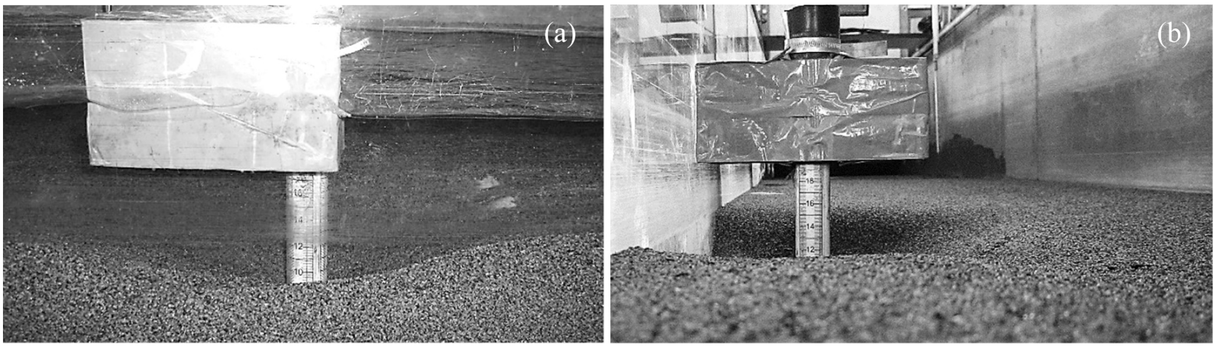

Fig. 2. Pictures of Test 55 (debris type A). Particular of **(a)** the debris during the test and **(b)** the scour equilibrium configuration at the end of the test.

RESULTS AND DISCUSSION

Dimensional analysis

In this section, the main non-dimensional parameters governing the scour depth evolution at bridge pier will be identified and empirical relationships will be derived. To do so, we based our dimensional analysis on earlier studies conducted by Melville and Chiew (1999) and Pagliara and Carnacina (2011) and introduced the parameter p_p to take into account the distance of the pier from the channel wall. Therefore, for reference tests, the maximum scour depth at bridge pier z_{max} can be expressed as a function of: 1) bridge pier and channel geometry (D, S_{hp}, b, p_p), with S_{hp} indicating the shape of the pier; 2) flow characteristics (q, h, ν, ρ), where q is the unit discharge, ν is the kinematic viscosity of water and ρ is the water density; 3) bed material characteristics (d_{50}, σ, Δ), with $\Delta = (\rho_s - \rho)/\rho$ indicating the sediment relative density and ρ_s the sediment density; 4) time t; and 5) gravity acceleration g:

$$z_{max} = f(D, S_{hp}, b, p_p, q, h, \nu, \rho, g, d_{50}, \sigma, \Delta, t) \tag{1}$$

Assuming q, ρ and d_{50} as repeating variables, in principle we should obtain eleven non-dimensional groups, i.e., the non-dimensional maximum scour depth z_{max}/D should depend on ten non-dimensional parameters. Nevertheless, the number of the governing parameters can be significantly reduced by considering that: 1) the effect of the parameter D/d_{50} on z_{max}/D is negligible in the tested range (Melville, 1997; Raudkivi and Ettema, 1983); 2) z_{max}/D does not depend on the Reynolds number $R_e = (4Uh)/\nu$ for tested flow conditions (Franzetti et al., 1989, 1994); 3) no armoring effect occurs for selected channel bed material ($\sigma < 1.3$); 4) U/U_c is kept constant in all of the tests; 5) z_{max}/D does not depend on S_{hp} as all of the tests were conducted with a cylindrical pier; 6) the effect of the parameter D/b on z_{max}/D is negligible for the adopted experimental apparatus (Shen et al., 1969); 7) one granular bed material was used for channel bed, i.e., σ and Δ are constant. Therefore, the governing functional relationship (for reference tests) can be written as follows:

$$\frac{z_{max}}{D} = \left(\frac{h}{D}, T^*, \frac{p_p}{b}\right) \tag{2}$$

where $T^* = (hUt)/(hD)$ is the non-dimensional time.

The presence of debris modifies the functional relationship Eq. (1) as four additional variables should be taken into consideration, i.e., d_d, t_d, l_d and S_{hd}, where S_{hd} is the debris shape. Therefore, for tests with LD accumulation, Eq. (1) can be generalized as follows (Pagliara and Carnacina, 2010):

$$z_{max} = f(D, S_{hp}, b, p_p, q, h, \nu, \rho, g, d_{50}, \sigma, \Delta, t, d_d, t_d, l_d, S_{hd}) \tag{3}$$

Following the dimensional analysis conducted for Eq. (2), four additional non-dimensional parameters can be derived, i.e., d_d/b, l_d/b, ΔA and S_{hd}. Among these, only the parameter ΔA affects the variable z_{max}/D. In fact, it can be observed that: 1) the shape of the debris is the same for both Type A and B; 2) the effect of the parameter d_d/b is negligible in the tested range, as well as 3) the effect of the parameter l_d/b (Pagliara and Carnacina, 2011). Thus, for scour at pier with LD accumulation Eq. (2) becomes:

$$\frac{z_{max}}{D} = \left(\frac{h}{D}, T_d^*, \frac{p_p}{b}, \Delta A\right) \tag{4}$$

where $T^*_d = (hUt)/[(d_d - D)t_d + hD]$ is the non-dimensional time (Pagliara and Carnacina, 2010). Note that $T^*_d = T^*$ for reference tests, as $d_d = D$ in the absence of LD accumulation.

Temporal evolution for reference configuration

For reference tests and symmetrically located pier, Kothyari et al. (1992), Oliveto and Hager (2002) and Pagliara and Carnacina (2010) observed that the scour evolution follows a logarithmic law. In particular, Pagliara and Carnacina (2010) and (2011) showed that the scour evolution is characterized by a linear trend in a semi-logarithmic chart, and its slope depends on U/U_c and h/D. Therefore, they introduced the temporal scour evolution parameter ξ and re-arranged Eq. (2) as follows:

$$\frac{z_{max}}{D} = \xi \ln\left(\frac{T^*}{10}\right) \tag{5}$$

In agreement with the findings of Melville (1997), Pagliara and Carnacina (2010) observed a slight dependence of ξ on the parameter h/D for $p_p/b = 0.5$ and $h/D > 2$, i.e., ξ can be expressed as only function of U/U_c. Conversely, the scour evolution is influenced by h/D for $h/D < 2$, thus resulting in $\xi\,(h/D, U/U_c)$.

Based on this observation and considering that present reference tests were conducted for $U/U_c \approx 1$ (i.e., U/U_c is constant), $1.05 \le h/D \le 5.67$ and $1/12 \le p_p/b \le 1/2$, the functional relationship proposed by Pagliara and Carnacina (2010) can be re-arranged as follows:

$$\xi = f\left(\frac{h}{D}, \frac{p_p}{b}\right) \tag{6}$$

Data analysis was conducted in steps. The first step aimed at understanding the effect of the variable p_p/b on z_{max}/D.

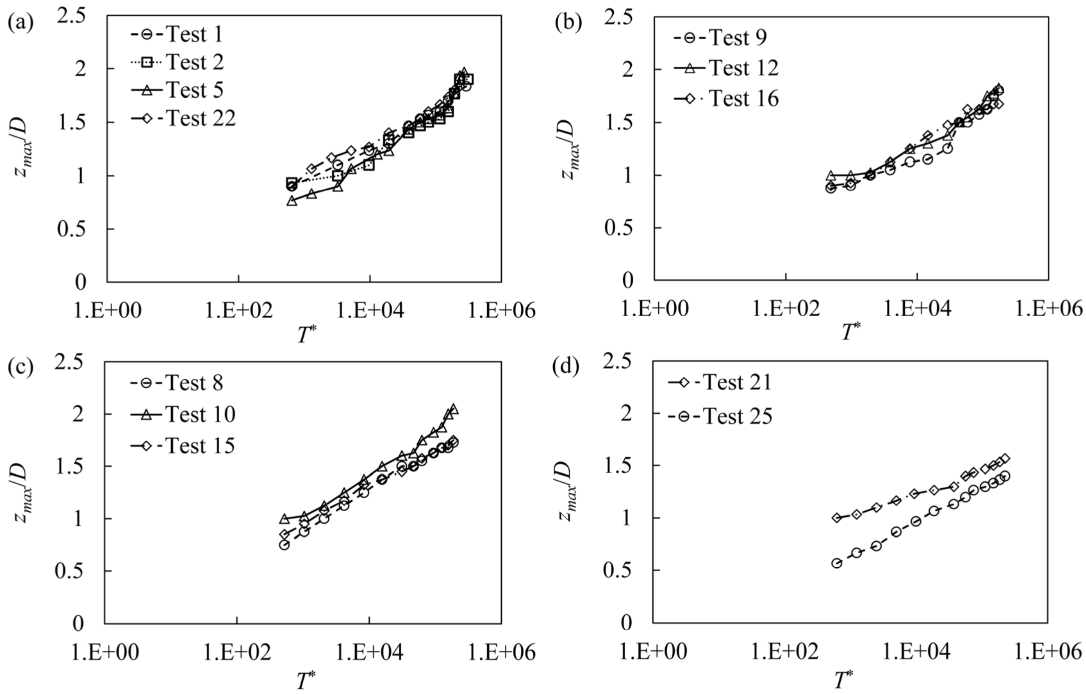

Fig. 3. Relationships z_{max}/D *vs.* T^* for different p_p/b values and **(a)** h/D = 5.67, **(b)** h/D = 4.25, **(c)** h/D = 2.00, and **(d)** h/D = 1.40.

Therefore, data points relative to selected tests were plotted in graphs $(z_{max}/D)(T^*)$, for different p_p/b values (Fig. 3). More specifically, Figs 3c and 3d reveal that the role of the parameter p_p/b is more prominent for $h/D < 2$, thus confirming the findings of previous studies relative to symmetrically located piers (Melville, 1997; Pagliara and Carnacina, 2010). Whereas, z_{max}/D does not depend on p_p/b for higher values of the parameter h/D (see Figs 3a and 3b). Such behavior can be reasonably explained considering that flow acceleration occurring in the region between the pier and the channel wall is more significant for lower tailwater. In fact, a more longitudinally extended scour morphology at equilibrium takes place in correspondence with the channel wall for lower h/D and p_p/b values, reflecting an increase of shear stress acting in such region of the channel.

Based on these observations, the second step of the data analysis aimed at finding the functional dependence of the variable ξ on h/D and p_p/b. To do so, 13 selected tests were chosen to calibrate the empirical expressions of ξ appearing in Eq. (5). It is worth noting that we have several values of $\xi(t)$, corresponding to the scour depth measurements $z_{max}(t)$ taken during each test. The analysis was limited to $T^* > 800$ (approximately corresponding to t ranging between 30 s and 60 s), as the scour evolution is highly uncertain in the very first developing phase (Pagliara and Carnacina, 2010). Data analysis allowed us to corroborate that $\xi(t)$ values pertaining to each test are very similar. Therefore, we can reasonably assume the average value ξ_{av} of each test for the following elaborations.

Figure 4 shows that ξ_{av} only depends on p_p/b and the effect of h/D is negligible for $h/D \geq 2$. In addition, ξ_{av} values for $h/D < 2$ exhibit a similar trend but are generally lower. In both the cases, the interpolating lines are characterized by the same slope and ξ_{av} can be expressed as $\xi_{av} = a(p_p/b) + c$, where a and c are coefficients. By assuming a linear variation of the coefficient c with h/D for $1.05 \leq h/D \leq 2$, we obtain:

$$\xi_{av} = -0.031\frac{p_p}{b} + 0.194 \tag{7}$$

valid for $1/12 \leq p_p/b \leq 1/2$ and $2 < h/D \leq 5.67$ (R^2 = 0.87), and

$$\xi_{av} = -0.031\frac{p_p}{b} + \left(0.036\frac{h}{D} + 0.122\right) \tag{8}$$

valid for $1/12 \leq p_p/b \leq 1/2$ and $1.05 \leq h/D \leq 2$ (R^2 = 0.94).

It is worth noting that Eq. (7) and (8) are analytically consistent, as the coefficient c of Eq. (8) is equal to 0.194 for h/D = 2. Thus, Eq. (5) becomes the general predicting equation, in which $\xi = \xi_{av}$ calculated either using Eq. (7) or Eq. (8) depending on the value of the parameter h/D.

Then, Eq. (5) was tested using all data of present study. Figure 5a shows the comparison between measured and calculated values (using Eq. (5)) of the variable z_{max}/D at different instants. Furthermore, we also tested Eq. (5) with data of Ettema et al. (2006), Sheppard et al. (2004), and Wang et al. (2016). It is worth noting that other authors' data pertain to tests conducted for p_p/b = 1/2, $0.8 < U/U_c < 0.96$ and $0.3 < h/D < 15.6$. Therefore, a slight over-estimation of the equilibrium non-dimensional scour depth should be expected for lower U/U_c values. In Fig. 5b, we contrasted the ratio $z_{max\ meas}/z_{max\ calc}$ with U/U_c, evidencing that the calculated value of the maximum scour depth ($z_{max\ calc}$) converges to measured value of the maximum scour depth ($z_{max\ meas}$) for $U/U_c \approx 1$.

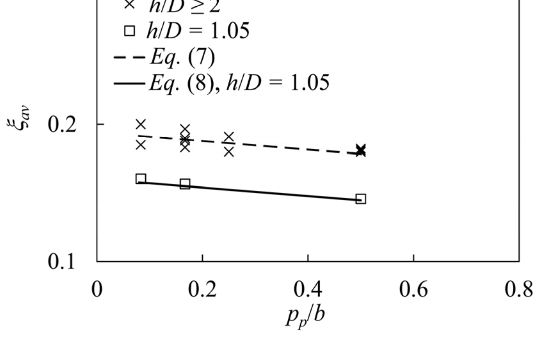

Fig. 4. ξ_{av} (p_p/b) for $h/D \geq 2.00$ and h/D = 1.05.

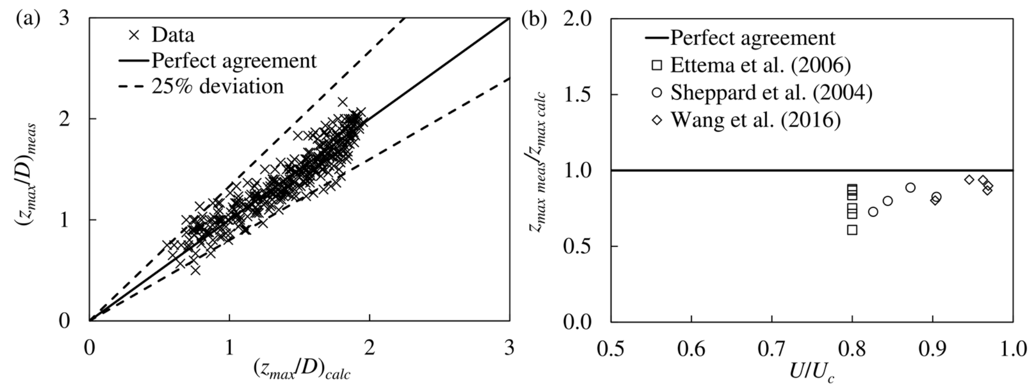

Fig. 5. **(a)** Comparison between measured and calculated values (using Eq. (5)) of the variable z_{max}/D at different instants; **(b)** $(z_{max\ meas}/z_{max\ calc})(U/U_c)$ for data at *equilibrium* derived from Ettema et al. (2006), Sheppard et al. (2004) and Wang et al. (2016).

Temporal evolution with LD accumulation

56 tests were carried out with LD accumulation at the pier under different water depths, percentage blockage ratios and the pier locations. Based on the dimensional considerations reported above and in agreement with the findings of Kothyari et al. (1992) and Oliveto and Hager (2002), Eq. (4) can be re-written as follows:

$$\frac{z_{max}}{D}=\xi' \ln\left(\frac{T_d^*}{10}\right) \tag{9}$$

where the scour evolution parameter ξ' can be expressed as:

$$\xi'=f\left(\frac{h}{D},\frac{p_p}{b},\Delta A\right) \tag{10}$$

For $p_p/b = 0.5$, Pagliara and Carnacina (2010) showed that the scour evolution in presence of LD does not depend on the parameter relative water depth for $2.67 \le h/D \le 5.67$. Therefore, they proposed the following equation to estimate ξ':

$$\xi' = 0.1835\left(\frac{U}{U_c}\Delta A^{0.4}\right) - 0.0986 \tag{11}$$

valid for $2.67 \le h/D \le 5.67$, $0.6 \le U/U_c \le 1$, and $5.4 \le \Delta A \le 12.1$.

As mentioned, the ranges of variation of the parameters h/D and ΔA are $1.40 \le h/D \le 5.67$ and $6 \le \Delta A \le 18$ for present tests with LD accumulation. Therefore, following the approach adopted for reference tests, tests were distinguished into two groups according to the value of the parameter h/D, i.e., for $1.40 \le h/D \le 2.0$ and $2.0 < h/D \le 5.67$. Data points pertaining to selected tests belonging to the two distinguished groups were plotted in Fig. 6. Namely, Fig. 6a shows $(z_{max}/D)(T_d^*)$ for $h/D = 5.67$ and Figs 6b and 6c show the same for $h/D = 2.67$ and for $h/D = 1.40$, respectively.

In addition, tests were selected in order to highlight the effects of the parameters p_p/b and ΔA. For example, in Fig. 6b, we report data points pertaining to tests 31 and 49. Such tests are characterized by the same ΔA but different p_p/b. It is apparent that the effect of the parameter p_p/b is negligible in terms of temporal evolution. But, the comparison between data point relative to tests 46, 49 and 52 evidences a significant increase of the scour depth with ΔA. Same considerations apply for tests reported in Figs 6a and 6c.

Likewise, the effect of the parameter h/D on $z_{max}/D(T_d^*)$ appears to be negligible for $2.0 < h/D \le 5.67$. In this regard, it is worth comparing the values of z_{max} for tests 28 and 29 and tests 31 and 32 in Figs 6a and 6b. Such values result to be very close, thus confirming the findings of Pagliara and Carnacina (2010).

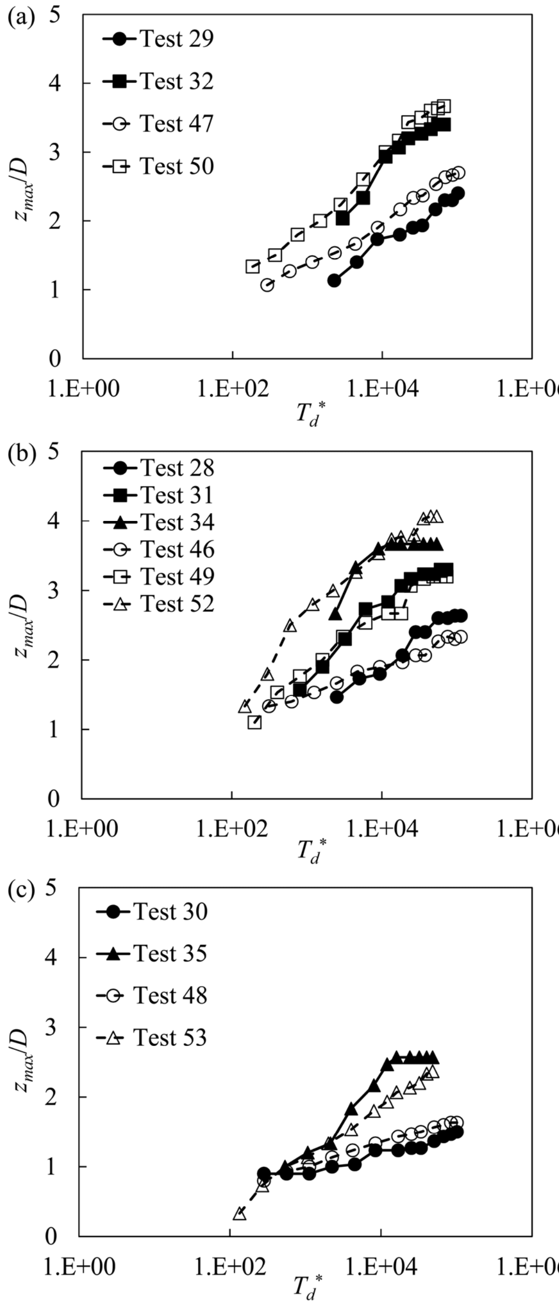

Fig. 6. $(z_{max}/D)(T_d^*)$ for different p_p/b and ΔA values with **(a)** $h/D = 5.67$, **(b)** $h/D = 2.67$, and **(c)** $h/D = 1.40$.

Conversely, a significant effect of h/D can be pointed out for $1.40 \leq h/D \leq 2.0$. In fact, z_{max}/D decreases with h/D, as clearly shown by Fig. 6c. For example, by comparing the values of z_{max} pertaining to tests 46, 47 and 48, a significant reduction of the maximum scour depth can be observed for test 48.

As for the role of the parameter p_p/b on scour depth evolution with LD accumulation, experimental evidences suggest a different behaviour with respect to that observed for reference tests. Namely, the effect of p_p/b on z_{max}/D is negligible for all tested conditions. This occurrence is essentially due to the modification of the flow characteristics caused by the debris, which results to be much more significant than that due to the pier position. In this regard, it is worth noting that equilibrium morphologies of tests with same ΔA and h/D values are characterized by similar features, reflecting a similar distribution of shear stresses acting on the granular bed.

Based on these observations and following the analysis methodology adopted for reference tests, 8 plus 15 tests were selected to calibrate the scour evolution parameter ξ' appearing in Eq. (11) for $1.40 \leq h/D \leq 2.0$ and $2.0 < h/D \leq 5.67$, respectively. Also in this case, each test is characterized by several values of $\xi'(t)$, corresponding to the measured scour depth $z_{max}(t)$. For each test, the values of $\xi'(t)$ (calculated assuming $U/U_c = 1$) were found to be very similar, allowing us to assume an average value ξ'_{av} for the following elaborations.

Figure 7 shows $\xi'_{av}(\Delta A^{0.4})$ and corroborates the negligibility of the parameter p_p/b on the evolution process. Namely, Fig. 7a evidences that Eq. (12) proposed by Pagliara and Carnacina (2010) also applies for present tests with LD accumulation and is valid for $U/U_c = 1$, $1/6 \leq p_p/b \leq 1/2$, $6 \leq \Delta A \leq 18$ and $2 < h/D \leq 5.67$ ($R^2 = 0.87$).

$$\xi'_{av} = 0.1835\Delta A^{0.4} - 0.0986 \tag{12}$$

Conversely, ξ'_{av} decreases with h/D for lower tailwater depths (Fig. 7b). By assuming a linear variation of ξ'_{av} with h/D, the following Eq. (13) ($R^2 = 0.87$) can be derived:

$$\xi'_{av} = \left(0.1762\frac{h}{D} - 0.1688\right)\Delta A^{0.4} + \left(-0.2365\frac{h}{D} + 0.3744\right) \tag{13}$$

and is valid for $U/U_c = 1$, $1/6 \leq p_p/b \leq 1/2$, $6 \leq \Delta A \leq 18$ and $1.40 \leq h/D \leq 2$. Note that Eqs. (12) and (13) are consistent, i.e., by substituting $h/D = 2$ in Eq. (13) we obtain the same coefficients of Eq. (12). Therefore, by assuming $\xi' = \xi'_{av}$ given either by Eq. (12) or Eq. (13) in Eq. (9), we obtain a general predicting equation to estimate the evolution of the maximum scour depth at bridge pier with LD accumulation. Figure 8 shows the comparison between measured and calculated values (using Eq. (9)) of the variable z_{max}/D at different instants for all the tests conducted in the present study.

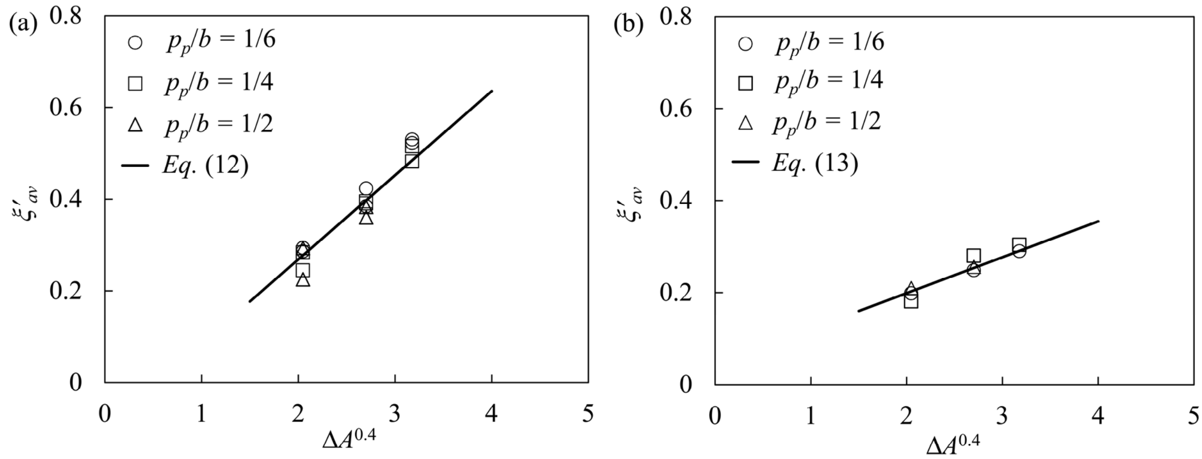

Fig. 7. $\xi'_{av}(\Delta A^{0.4})$ for different p_p/b values and **(a)** $2 < h/D \leq 5.67$ and **(b)** $h/D = 1.40$.

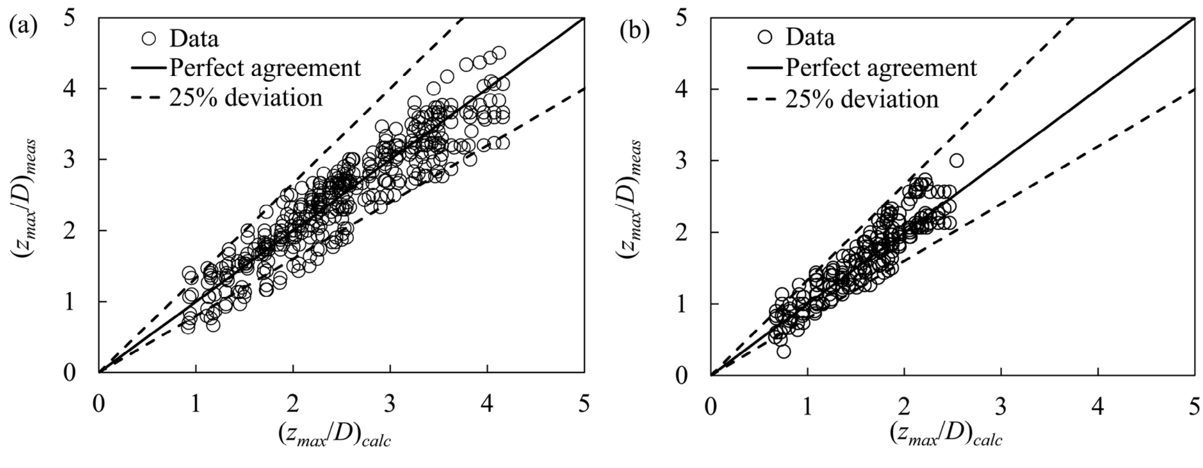

Fig. 8. Comparison between measured and calculated values (using Eq. (9)) of the variable z_{max}/D at different instants for **(a)** $2 < h/D \leq 5.67$ and **(b)** $1.04 \leq h/D \leq 2$.

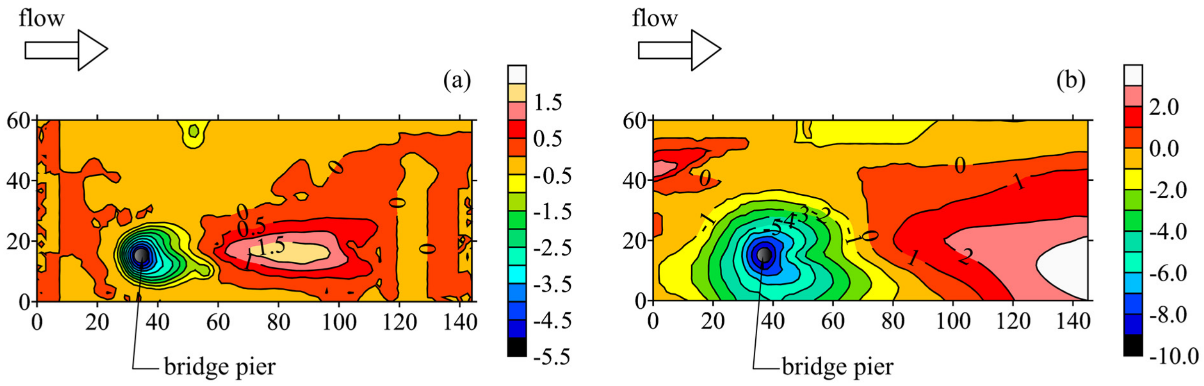

Fig. 9. Equilibirum morphologies for test **(a)** 2 and **(b)** 32. Units of the legend and axes are expressed in cm.

Overall, the presence of LD accumulation has negligible effect on the location of the maximum scour depth, that occurs in correspondence with the upstream side of the pier, regardless of the debris characteristics. But it contributes to deeply modify the equilibrium morphology, involving all scour features (i.e., area, volume, length, width and depth). Figure 9 shows two examples of equilibrium morphologies pertaing to Test 2 and 32. They are characterized by identical hydraulic conditions and pier position. It can be observed that the presence of the LD accumulation in test 32 results in a scour depth that is almost double than that of test 2. In addition, the scour formation reaches the channel wall. In this regard, the present analysis provides some interesting and unprecedented information that can be helpful for hydraulic engineers. It is worth noting that the configurations investigated in this study usually occur in natural contexts. For example, in curved river branches, floating debris can easily accumulate in correspondence with bridge piers. Therefore, the estimation of maximum scour depth is essential not only to correctly design pier foundation, but also to reduce the risk of bank failure.

Finally, as this is the first study analyzing the combined effect of pier distance from the channel wall and LD accumulation on scour at bridge pier, different pier diameters were used. Based on experimental evidences, it is reasonable to assume that no substantial differences in terms of scour mechanism could be pointed out for $D/b \leq 0.1$. However, for $D/b>0.1$, there could be a contraction effect, resulting in an increase of the scour depth, all other parameters being constant. Therefore, further tests are needed to investigate such effect. Likewise, a more comprehensive analysis could be performed by varying the roughness, shape and percentage blockage ratio of the LD accumulation.

CONCLUSIONS

The effect of bridge pier distance from the channel wall on the scour evolution was investigated with and without large debris accumulation. Two different debris types and three percentage blockage ratios were tested. Data analysis revealed that pier location influences the maximum equilibrium scour depth and its evolution only in the case of isolated pier, whereas its effect becomes negligible in the presence of large debris accumulation. As for the flow depth, we corroborated the findings of other studies, evidencing that low relative tailwaters significantly influence scour evolution and equilibrium condition for all the tested configurations. Conversely, scour mechanism slightly depends on this parameter for higher water depths. Empirical equations were developed to predict both the scour depth at equilibrium and its evolution in the tested range of parameters. Such equations were also tested with data at equilibrium of other authors, showing a satisfactory predicting capability regardless the different tested conditions. Further investigations are needed to explore the effect of flow characteristics on scour process when the approaching flow velocity is lower than the critical velocity.

Acknowledgements. Authors wish to thank the technicians of the hydraulics laboratory of the University of Pisa, Mr. Nicola Bruni, Mr. Antonio Cecchi, Mr. Alessandro Michelotti, and Mr. Vincenzo Pennabea for their help in building the experimental apparatus. This research did not receive any specific grant from funding agencies in the public, commercial, or not-for-profit sectors.

Conflicts of interest. The authors confirm that they have no potential conflicts of interest.

Data availability statement. The authors confirm that the data supporting the findings of this study are available within the article.

REFERENCES

Abbe, T.B., Montgomery, D.R., 2003. Patterns and processes of wood debris accumulation in the Queets river basin, Washington. Geomorphology, 51, 81–107. DOI: 10.1016/S0169-555X(02)00326-4

Andreoli, A., Comiti, F., Lenzi, M.A., 2007. Characteristics, distribution and geomorphic role of large woody debris in a mountain stream of the Chilean Andes. Earth. Surf. Process. Landf., 32, 1675–1692. DOI: 10.1002/esp.1593

Barbhuiya, A.K., Dey, S., 2003. Vortex flow field in a scour hole around abutments. Int. J. Sediment. Res., 18, 310–325.

Bradley, J.B., Richards, D.L., Bahner, C.D., 2005. Debris Control Structures – Evaluation and Countermeasures (Report No. FHWA-IF-04-016, Hydraulic Engineering No. 9, 3th edition). Federal Highway Administration, Washington, D.C.

Braudrick, C.A., Grant, G.E., 2001. Transport and deposition of large woody debris in streams: a flume experiment. Geomorphology, 41, 263–283. DOI: 10.1016/S0169-555X(01)00058-7.

Briaud, J.L., Chen, H.C., Chang, K.A., Chen, X., Oh, S.J., 2006. Scour at bridges due to debris accumulation: a review. In: Proceedings of 3rd International Conference on Scour and Erosion. Amsterdam, The Netherlands, pp. 113–120.

Chang, W.Y., Lai, J.S., Yen, C.L., 2004. Evolution of scour depth at circular bridge piers. J. Hydraul. Eng., 130, 905–913. DOI: 10.1061/(ASCE)0733-9429(2004)130:9(905)

Chiew, Y.M., 1995. Mechanics of riprap failure at bridge piers. J. Hydraul. Eng., 121, 635–643. DOI: 10.1061/(ASCE)0733-9429(1995)121:9(635)

Dey, S., 1999. Time variation of scour in the vicinity of circular piers. In: Proceedings of the Institution of Civil Engineers: Water, Maritime & Energy. 136, 67–75. DOI: 10.1680/iwtme.1999.31422

Dey, S., Barbhuiya, A.K., 2005. Time variation of scour at abutments. J. Hydraul. Eng., 131, 11–23. DOI: 10.1061/(ASCE)0733-9429(2005)131:1(11)

Diehl, T.H., 1997. Potential Drift Accumulation at Bridges (Report FHWA–RD–97–028, Hydraulic Engineering No. 9). Federal Highway Administration, Washington, D.C.

Ettema, R., Kirkil, G., Muste, M., 2006. Similitude of large-Scale turbulence in experiments on local scour at cylinders. J. Hydraul. Eng., 132, 33-40. DOI: 10.1061/(ASCE)0733-9429(2006)132:1(33)

Franzetti, S., Larcan, E., Mignosa, P., 1989. Erosione alla base di pile circolari di ponte: verifica sperimentale dell'ipotesi di esistenza di una situazione finale di equilibrio. Idrotecnica, 16, 135–141. (In Italian.)

Franzetti, S., Malavasi, S., Piccinin, C., 1994. Sull'erosione alla base delle pile dei ponti. In: 14th Convegno d'Idraulica e Costruzioni Idrauliche. Naples, Italy, pp. 13-24. (In Italian.)

Gurnell, A.M., Piégay, H., Swanson, F.J., Gregory, S.V., 2002. Large wood and fluvial processes. Freshw. Biol., 47, 601–619. DOI: 10.1046/j.1365-2427.2002.00916.x

Hagerty, D.J., Parola, A.C., Fenske, T.E., 1995. Impacts of 1993 upper Mississippi River Basin Floods on Highway Systems (Report No. 1483). Transportation Research Record. Transportation Research Board, Washington, D.C.

Kandasamy, J.K., Melville, B.W., 1998. Maximum local scour depth at bridge piers and abutments. J. Hydraul. Res., 36, 183–198. DOI: 10.1080/00221689809498632

Kattell, J., Eriksson, M., 1998. Bridge Scour Evaluation: Screening, Analysis, and Countermeasures (General Technical Report 9877 1207–SDTDC). U.S. Department of Agriculture, Forest San Dimas, CA.

Kothyari, U.C., Garde, R.J., Ranga Raju, K.G., 1992. Temporal variation of scour around circular bridge piers. J. Hydraul. Eng., 118, 1091–1106. DOI: 10.1061/(ASCE)0733-9429(1992)118:8(1091)

Laursen, E.M., 1958. Scour at Bridge Crossings (Bulletin No. 8). Iowa Highways Research Board, Ames, Iowa.

Link, O., Pfleger, F., Zanke, U., 2008. Characteristics of developing scour-holes at a sand-embedded cylinder. Int. J. Sediment. Res., 23, 258–266. DOI: 10.1016/S1001-6279(08)60023-2

Lyn, D.A., Cooper, T., Yi, Y.K., Sinha, R., Rao, A.R., 2003. Debris Accumulation at Bridge Crossings: Laboratory and Field Studies (Report FHWA/IN/JTRP-2003/10). INDOT Division of Research, West Lafayette, IN.

Masjedi, A., Shafaei-Bejestan, M., Esfandi, A., 2010. Experimental study on local scour around single oblong pier fitted with a collar in a 180 degree flume bend. Int. J. Sediment. Res., 25, 304–312. DOI: 10.1016/S1001-6279(10)60047-9

Melville, B.W., 1997. Pier and abutment scour: Integrated approach. J. Hydraul. Eng., 123, 125–136. DOI: 10.1061/(ASCE)0733-9429(1997)123:2(125)

Melville, B.W., Chiew, Y.M., 1999. Time scale for local scour at bridge piers. J. Hydraul. Eng., 125, 59–65. DOI: 10.1061/(ASCE)0733-9429(1999)125:1(59)

Melville, B.W., Coleman, S.E., 2000. Bridge Scour. Water Resources Publications, LLC, Colorado, U.S.A.

Melville, B.W., Dongol, D.M., 1992. Bridge pier scour with debris accumulation. J. Hydraul. Eng., 118, 1306–1310. DOI: 10.1061/(ASCE)0733-9429(1992)118:9(1306)

Melville, B.W., Sutherland, A.J., 1988. Design method for local scour at bridge piers. J. Hydraul. Eng., 114, 1210–1226. DOI: 10.1061/(ASCE)0733-9429(1988)114:10(1210)

Mueller, D.S., Parola, A.C., 1998. Detailed scour measurements around a debris accumulation. In: Proceedings of International Water Resources Engineering Conference. Reston, VA, pp. 234–239.

Oliveto, G., Hager, W.H., 2002. Temporal evolution of clear–water pier and abutment scour. J. Hydraul. Eng., 128, 811–820. DOI: 10.1061/(ASCE)0733-9429(2002)128:9(811)

Oliveto, G., Hager, W.H., 2005. Further results to time–dependent local scour at bridge elements. J. Hydraul. Eng., 131, 97–105. DOI: 10.1061/(ASCE)0733-9429(2005)131:2(97)

Pagliara, S., Carnacina, I., 2010. Temporal scour evolution at bridge piers: effect of wood debris roughness and porosity. J. Hydraul. Res., 48, 3–13. DOI:10.1080/00221680903568592.

Pagliara, S., Carnacina, I., 2011. Influence of wood debris accumulation on bridge pier scour. J. Hydraul. Eng., 137, 254–261. DOI: 10.1061/(ASCE)HY.1943-7900.0000289

Pagliara, S., Palermo, M., Azizi, R., 2015. Scour control at bridge piers using macro-roughness elements. In: Proceedings of the Institution of Civil Engineers: Water Management. 168, pp. 174–188. DOI: 10.1680/wama.14.00006

Parola, A.C., Apelt, C.J., Jempson, M.A., 2000. Debris Forces on Highway Bridges (NCHRP Report No. 445). Transportation Research Record, Transportation Research Board, Washington, D.C.

Parola, A.C., Kamojjala, S., Richardson, J., Kirby, M., 1998. Numerical simulation of flow patterns at a bridge with debris. In: Proceedings of International Water Resources Engineering Conference. Reston, VA, pp. 240–245.

Raikar, R.V., Dey, S., 2008. Kinematics of horseshoe vortex developing in an evolving scour hole at a square cylinder. J. Hydraul. Res., 46, 247–264. DOI: 10.1080/00221686.2008.9521859

Raudkivi, A.J., Ettema, R., 1983. Clear-water scour at cylindrical piers. J. Hydraul. Eng., 109, 338–350. DOI: 10.1061/(ASCE)0733-9429(1983)109:3(338)

Raudkivi, A.J., Ettema, R., 1985. Scour at cylindrical bridge piers in armoured beds. J. Hydraul. Eng., 111, 713–731. DOI:10.1061/(ASCE)0733-9429(1985)111:4(713).

Richardson, E.V., Davis, S.R., 2001. Evaluating Scour at Bridges (Report No. FHWA–NHI–01–001, Hydraulic engineering No. 18, 4th edition). Federal Highway Administration, Washington, D.C.

Shen, H.W., Schneider, V.R., Karaki, S.S., 1969. Local scour around bridge piers. J. Hydraul. Div. (ASCE), 95, 1919–1940.

Sheppard, D.M., 1999. Conditions of maximum local scour. In: Richardson, E.V., Lagasse, P.F. (Eds.): Stream Stability and Scour at Highway Bridges. ASCE, pp. 347–364.

Sheppard, D.M., Odeh, M., Glasser, T., 2004. Large scale clear-water local pier scour experiments. J. Hydraul. Eng., 130, 957–963. DOI: 10.1061/(ASCE)0733-9429(2004)130:10(957)

Tang, H.W., Ding, B., Chiew, Y.M., Fang, S.L., 2009. Protection of bridge piers against scouring with tetrahedral frames. Int. J. Sediment. Res., 24, 385–399. DOI: 10.1016/S1001-6279(10)60012-1

Wallerstein, N., Thorne, C.R., 1996. Impact of Woody Debris on Fluvial Processes and Channel Morphology in Stable and Unstable Streams. Department of Geography, University of

Nottingham, Nottingham, UK.
Wang, H., Tang, H., Liu, Q., Wang, Y., 2016. Local scouring around twin bridge piers in open-channel flows. J. Hydraul. Eng., 142, 1–8. DOI: 10.1061/(ASCE)HY.1943-7900.0001154
Wu, W., Wang, S.S.Y., 1999. Movable bed roughness in alluvial rivers. J. Hydraul. Eng., 125, 1309-1312. DOI: 10.1061/(ASCE)0733-9429(1999)125:12(1309)
Zarrati, A.R., Chamani, M.R., Shafaie, A., Latifi, M., 2010. Scour countermeasures for cylindrical piers using riprap and combination of collar and riprap. Int. J. Sediment. Res., 25, 313–321. DOI: 10.1016/S1001-6279(10)60048-0
Zevenbergen, L.W., 2000. Time scale for contraction scour at bridges. In: Proceedings of Joint Conference on Water Resources Engineering and Water Resources Planning & Management. Minneapolis.
Zevenbergen, L.W., Lagasse, P.F., Clopper, P.E., Spitz, W.J., 2006. Effect of debris on bridge pier scour. In: Proceedings of the 3rd International Conference on Scour and Erosion. Amsterdam, The Netherlands, pp. 741–749.

Received 19 June 2020
Accepted 6 October 2020

NOMENCLATURE

a = coefficient (–)
b = channel width (m)
c = coefficient (–)
D = pier diameter (m)
d_{xx} = particle diameter for which xx% of material is finer (m)
d_d = debris width (m)
g = gravity acceleration (m s^{-2})
h = approach flow depth (m)
h_d = debris height (m)
i_c = energy line slope (–)
l_d = debris length (m)
n = Manning's coefficient (m$^{-1/3}$ s)
p_p = distance of the pier from channel wall (m)
q = unit discharge (m^2 s^{-1})
Q = discharge (m^3 s^{-1})
R^2 = determination coefficient (–)
$\mathrm{R_e}$ = Reynolds number (–)
S_{hd} = debris shape (–)
S_{hp} = bridge pier shape (–)
T^* = non dimensional time for reference tests (–)
T_d^* = non dimensional time for tests with debris accumulation (–)
t = time (s)
t^* = test duration (s)
t_d = debris submerged height (m)
u^*_c = the critical shear velocity (m s^{-1})
U = approach flow velocity (m s^{-1})
U_c = critical flow velocity (m s^{-1})
z_{max} = maximum scour depth at bridge pier (m)
$z_{max\ calc}$ = calculated maximum scour depth at bridge pier (m)
$z_{max\ meas}$ = measured maximum scour depth at bridge pier (m)
ΔA = percentage blockage ratio (–)
Δ = sediment relative density (–)
ξ = scour evolution parameter for reference tests (–)
ξ' = scour evolution parameter for tests with debris (–)
ξ_{av} = average scour evolution parameter for reference tests (–)
ξ'_{av} = average scour evolution parameter for tests with debris (–)
ν = kinematic viscosity of water (m^2 s^{-1})
ρ = water density (kg m^{-3})
ρ_s = sediment density (kg m^{-3})
σ = sediment uniformity (–)
θ = Shields' parameter (–)